Available online at www.sciencedirect.com

SciVerse ScienceDirect

Ceramics International 39 (2013) 5585–5590

CERAMICS INTERNATIONAL

www.elsevier.com/locate/ceramint

Microstructure of silicon-incorporated carbon films with various silicon concentrations deposited by hybrid magnetron sputtering/chemical vapor deposition

Hsin-Chung Cheng[a,b,c], Duen-Jeng Wang[b,c,1], Wen-Chien Lan[b,c], Pei-Yi Wang[c,d], Shih-Fu Ou[c,e], Ya-Ju Hsu[f], Keng-Liang Ou[c,e,g,*]

[a] *Division of Orthodontics, Department of Dentistry, Taipei Medical University Hospital, Taipei 110, Taiwan*
[b] *School of Dentistry, College of Oral Medicine, Taipei Medical University, Taipei 110, Taiwan*
[c] *Research Center for Biomedical Devices and Prototyping Production, Taipei Medical University, Taipei 110, Taiwan*
[d] *Department of Dental Technology, Taipei Medical University, Taipei 110, Taiwan*
[e] *Graduate Institute of Biomedical Materials and Tissue Engineering, College of Oral Medicine, Taipei Medical University, Taipei 110, Taiwan*
[f] *Department of Endodontics, Sijhih Cathay General Hospital, Taipei 221, Taiwan*
[g] *Research Center for Biomedical Implants and Microsurgery Devices, Taipei Medical University, Taipei 110, Taiwan*

Received 19 October 2012; received in revised form 19 December 2012; accepted 20 December 2012
Available online 28 December 2012

Abstract

A hybrid technique combining the radio-frequency magnetron sputtering of silicon and the plasma-enhanced chemical vapor deposition of hydrogenated carbon was developed to synthesize silicon-incorporating diamond-like carbon films. Plasma power was supplied at different levels to a silicon electrode in an Ar/CH_4 atmosphere to prepare films having different Si contents. The effects of plasma power level on the compositions and microstructures of the deposited film were investigated. The Si contents and deposition rates of the films increased with the plasma power. All the films exhibited an amorphous structure. The addition of Si not only resulted in the smoothening of the granular surfaces of the films but also led to the formation of round projections having a diameter of about 200 nm on the surfaces. Most of the Si in the films reacted with carbon, and no precipitation of SiC or Si phases was noticed in the films.

Keywords: A. Films; D. Carbon; E. Biomedical applications

1. Introduction

Amorphous hydrogenated diamond-like carbon (a-C:H) films have been used extensively as protective and functional coatings in industrial and biological applications owing to their good mechanical characteristics, biocompatibility, corrosion resistance, wear resistance, chemical inertness, smooth surfaces, ability to conduct heat, and noncytotoxic nature [1–6]. The properties of a-C:H films can be altered by incorporating additional elements such as F, N, O, Cu, Ti, Ag, and Si in various amounts [7–14]. Adding the nonmetallic elements F, N, and O can change the wear resistance, surface hardness, and hydrophilicity of a-C:H films. In addition, incorporating metallic elements can improve the biocompatibility and antimicrobial property of the films. However, some doping elements, such as Cu and Ag, are chemically inert to elemental C, and their solubilities in C are also very low, causing the elements to form a segregated metallic phase in the a-C:H matrix [10,15]. On the other hand, doping elements that react more readily with C, such as Ti and Si, can induce the carbide phase in the a-C:H films [11,14]. The formation of metallic and carbide phases results in the a-C:H films that exhibit differences in their mechanical characteristics,

---

[*] Corresponding author at: Graduate Institute of Biomedical Materials and Tissue Engineering, Taipei Medical University, Taipei 110, Taiwan. Tel.: +886 2 27361661x5100; fax: +886 2 27395524.
E-mail address: klou@tmu.edu.tw (K.-L. Ou).
[1] Co-first author. Duen-Jeng Wang

0272-8842/$ - see front matter © 2013 Elsevier Ltd and Techna Group S.r.l. All rights reserved.
http://dx.doi.org/10.1016/j.ceramint.2012.12.073

including corrosion resistances and surface morphologies, depending on the phase formed. In addition, the introduction of various doping elements having different chemical properties adds different functionalities to a-C:H films. For instance, it has been reported that the addition of elemental Si improved the thermal stability, resistance to corrosion in body fluids, and mechanical stability of a-C:H films, while also resulting in higher interfacial toughness and better biocompatibility [7,13,16]. Therefore, Si-incorporating a-C:H coatings have the potential to be used as protective layers for implants and other surgically placed medical devices.

The most commonly used low-temperature a-C:H film coating techniques, such as plasma-enhance chemical vapor deposition (PECVD) [13,17,18], ion-beam deposition [19], magnetron sputtering [20,21] and vacuum-arc deposition [22–25], all make use of plasma-based enhancement. The generation of plasma can effectively decompose the used hydrocarbon gas into carbon species, which can be used to synthesize a carbon film on the surface of the deposition substrate. The aim of this study was to combine the radio-frequency (RF) plasma deposition of a-C:H films and the magnetron sputtering-based deposition of silicon to synthesize silicon-incorporating a-C:H films in an atmosphere of argon and methane. The effects of the plasma power supplied to the Si sputtering electrode on the compositions and microstructures of the obtained films were investigated.

2. Materials and methods

The Si-incorporating a-C:H (Si/a-C:H) films were deposited on silicon wafers having a diameter of 1 cm and a thickness of 2 mm. All substrates were cleaned in an ultrasonic bath using the following cleaning sequence: 15 min in acetone, 10 min in deionized water, and finally, 15 min in ethanol. Then, the substrates were dried at 80 °C for 8 h in an oven and loaded into the deposition chamber. The deposition process used was a hybrid of the radio-frequency plasma chemical vapor deposition of a-C:H films and the magnetron sputtering of silicon. The plasma species generated between the sputtering gun and the substrate simultaneously sputtered Si atoms from the silicon electrode and decomposed the CH_4 gas, which was used as the carbon source, resulting in the synthesis of the composite films. The equipment setup and details of the deposition procedures have been described previously [9,26]. The distance between the silicon electrode and the substrates was fixed at 60 mm. After evacuating the chamber and heating the substrates to 200 °C, a methane/argon gas mixture in a ratio of 1/1.5 was introduced into the chamber and RF plasma was generated. To deposit films having different Si contents, plasma power was supplied for 10 min each at the following five levels: 100, 150, 200, 250, and 300 W.

Field-emission scanning electron microscopy (FESEM) (JSM-6500F) was employed to determine the surface morphologies and thicknesses of the deposited films. The crystallographic structures of the films were identified via transmission electron microscopy (TEM) (JEM-2100) using an operational voltage of 200 kV.The crystallinity and phase were identified via glancing angle X-ray diffraction (XRD) using a CuKα radiation with an incidence angle of 1° and at a scanning speed of 2°/min performed using a CuKα radiation source (SIEMENS D5000). X-ray photoelectron spectroscopy (XPS) (AES-650) was used to analyze the elemental bonds present in the films and to determine the chemical compositions of the films. Before XPS detection, the sample surface was cleaned by Ar^+ ion-beam bombardment.

3. Results and discussion

Fig. 1 shows the surface morphologies of the various a-C:H films having different Si contents. Unlike in the case of a-C:H films formed via PECVD, which have numerous

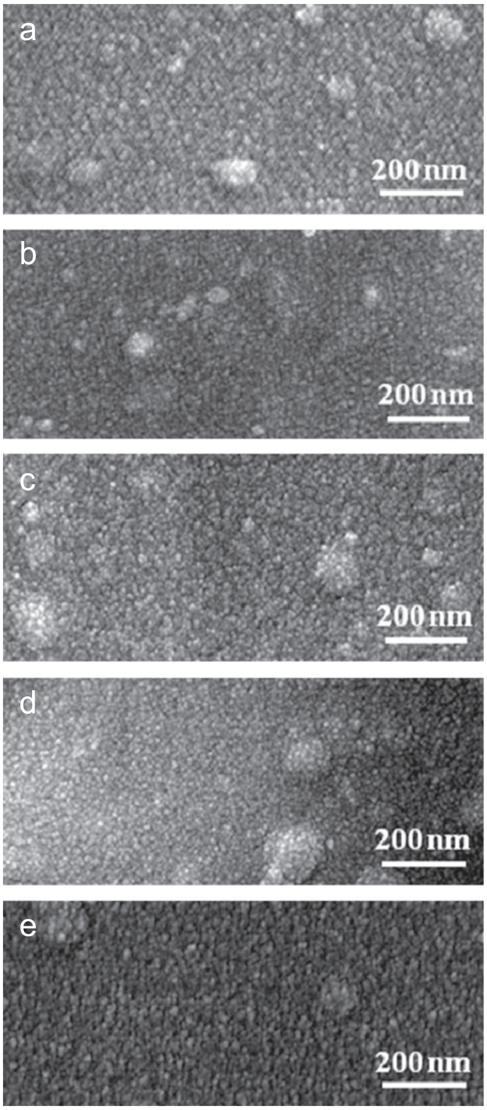

Fig. 1. SEM images of (a) a-C:H/$Si_{0.16}$ film, (b) a-C:H/$Si_{0.17}$ film, (c) a-C:H/$Si_{0.21}$film, (d) a-C:H/$Si_{0.24}$ film and (e) a-C:H/$Si_{0.49}$ film.

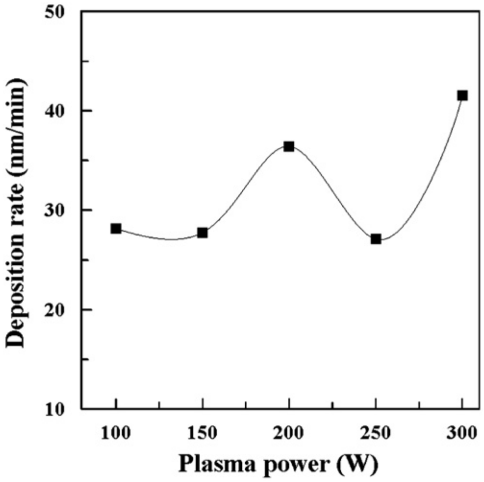

Fig. 2. Dependence of the film deposition rate as a function of plasma power.

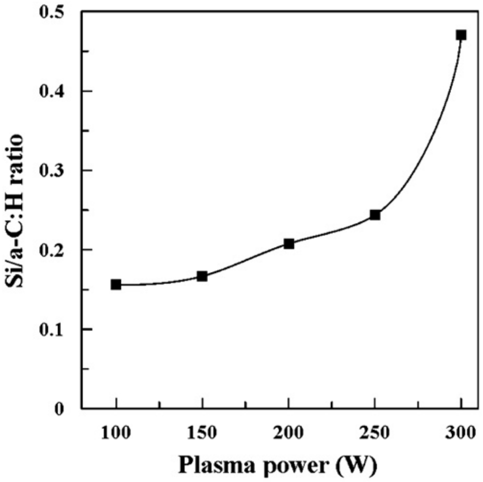

Fig. 3. Dependence of the Si/a-C:H ratio in film as a function of plasma power.

small ridges on their surfaces [27], a number of uniformly distributed sharp-edged granules were observed on the surfaces of the Si-incorporating a-C:H films. With an increase in the Si content, these granules became smaller. However, larger, round projections appeared on the film surfaces. This indicated that the roughness of the film surfaces changed with the Si content of the films. The deposition rates for the obtained films, shown in Fig. 2, were calculated by measuring their thicknesses. The deposition rate increased with an increase in the plasma power supplied. However, the increase was not linear and dissimilar to the linear dependence usually seen in the case of PECVD carbon films [28], where an increase in the plasma power supplied intensifies the decomposition of methane. However, this type of nonlinear dependence is common in reactive sputtering processes and is known to be the result of a phenomenon called the "target poisoning effect". An increase in the plasma power should intensify ion bombardment on the silicon electrode and cause a greater number of silicon species to eject, thus resulting in greater silicon deposition and thus a film of greater thickness. However, a carbide layer with a low sputtering yield forms on the silicon electrode and limits the ejection flux of the silicon species, consequently reducing the deposition rate. Even though the target poisoning effect can usually be suppressed by using a radio-frequency mode power supply, it can still cause a sudden drop in the deposition rate at a plasma power of 250 W. The film deposition rate is also affected by the dissociation of methane and the attachment of the plasma species. It has been reported that doping a-C:H films with Si enhances the formation of C–H$_n$ and Si–H$_n$ bonds in the films [13,29]. The formation of these bonds is also influenced by the dissociation of methane. Thus, it was assumed that the volume fraction of such single-bonded hydrogen atoms could also be an important factor affecting the film deposition rate.

The values of Si/a-C:H ratio, shown in Fig. 3, supported this assumption. The values of the Si/a-C:H ratio of the films deposited at plasma powers of 100 W, 150 W, 200 W, 250 W, and 300 W were 0.16, 0.17, 0.21, 0.24, and 0.49, respectively. These films are subsequently referred to as a-C:H/Si$_{0.16}$, a-C:H/Si$_{0.17}$, a-C:H/Si$_{0.21}$, a-C:H/Si$_{0.24}$, and a-C:H/Si$_{0.49}$, respectively. The value of the Si/a-C:H ratio increased exponentially with an increase in the plasma power. The curve of the values of the Si/a-C:H ratio dips slightly downward at 150 W and 250 W, with the dips partly confirming the reduction in the Si flux because of target poisoning. The lower silicon content in the films deposited at plasma power levels lower than 250 W indicated that the deposition rate at lower power levels was mainly determined not only by the level of the power supplied but also by the deposited a-C:H matrix. Most of the energy supplied was consumed by the complex interactions between the hydrocarbon molecules and the electrons. However, once the plasma power supplied was high enough, the emission rate and kinetic energy of the ions was sufficient to remove the carbide film formed on the surface of the silicon electrode. This resulted in a sudden increase in the flux of the silicon species, with the plasma power level now determining the deposition rate and the composition of the film deposited.

The chemical states of the carbon atoms in the a-C:H:Si films were determined using the C1s core level spectra of the films. The XPS spectra of the C1s core level of the deposited films, shown in Fig. 4, suggested that the primary bonds in the films were the C=C sp^2 (284.6 eV) and C–C sp^3 (285.4 eV) bonds. A few C–Si (283.7 eV) and CO- (286.6 eV) bonds were also seen to coexist in the films. The fraction ratio of the C=C sp^2 and C–C sp^3 bonds increased with the Si content of the films. This result was not in accordance with those reported in the case of Si-incorporating a-C:H films deposited via PECVD by Camargo et al. [13] and Iseki et al. [30]. They found that the incorporation of silicon inhibited cluster formation in the a-C:H phase owing to the opening up of the six-fold aromatic rings and the replacement of the carbon atoms

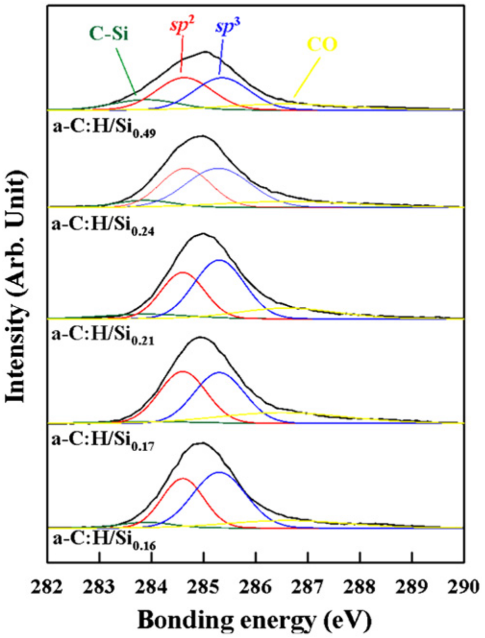

Fig. 4. XPS C1s spectra of a-C:H/Si films with different Si contents.

in the sp^2-bonded carbon clusters [31]. Considering the atomic structure of Si, which is known to form only four-fold-coordinated networks (Si-C), the number of Si–C bonds present should be included when determining the overall sp^3 bond fraction. Therefore, the values of the overall sp^2/sp^3 ratio of the films determined in this study were only approximate. Camargo et al. [13] had also suggested that hydrogen effusion caused by heating might be associated with the carbonization of the films and the conversion of hydrogenated sp^3 bonds into sp^2 bonds. Tai et al. had also obtained a similar result [32]. Thus, the higher temperatures to which the substrates were heated in this study might also have contributed to the carbonization of the deposited films. These two competing factors were responsible for the results of the current study being different from those previously reported. It is known that the number of sp^3 and sp^2 bonds present significantly affects the hardness of amorphous carbon materials, with a higher number of the former resulting in greater hardness [33,34]. However, the doping of silicon also increases the hydrogen content of a-C:H films, and this can increase the number of polymeric C–H$_n$ and Si–H$_n$ bonds. These polymeric bonds weaken the structural integrity of the films, reduce the stress produced, and consequently decrease the hardness of the films [29]. The voids remaining after hydrogen effusion also affect network connectivity in Si-rich a-C:H films and reduce the hardness of the films [31].

The presence of these complex mixed-type bonds indicated that the structure of the a-C:H matrix in all the films, which had different Si contents, was disordered. The XRD patterns of the Si-incorporating a-C:H films, shown in Fig. 5, supported this conclusion. All the films deposited and investigated in this study had a similar structure, which was amorphous. The only distinguishable diffraction peak in the XRD spectra of the films was that belonging to the Si of the wafer substrate. However, the XPS Si 2p spectra of the films, shown in Fig. 6, indicated the presence of Si–C (102.2 eV) bonds and Si–Si (101.1 eV) bonds in the films. The fraction ratios of the Si–C and Si–Si bonds increased with an increase in the Si content of the films. This result was similar to that reported by Zhao et al. [31]. The increase in the number of Si–C and Si–Si bonds implied that there might be SiC or Si phases present in the form of precipitates in the films with high Si contents. To further investigate the microstructures of these a-C:H/Si films, they were analyzed using TEM. As can be seen from the cross-sectional TEM image shown in Fig. 7, no obvious secondary phase was found in the

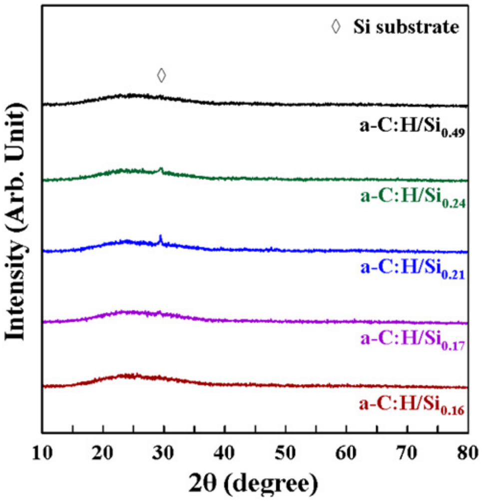

Fig. 5. XRD patterns of a-C:H/Si film coated samples.

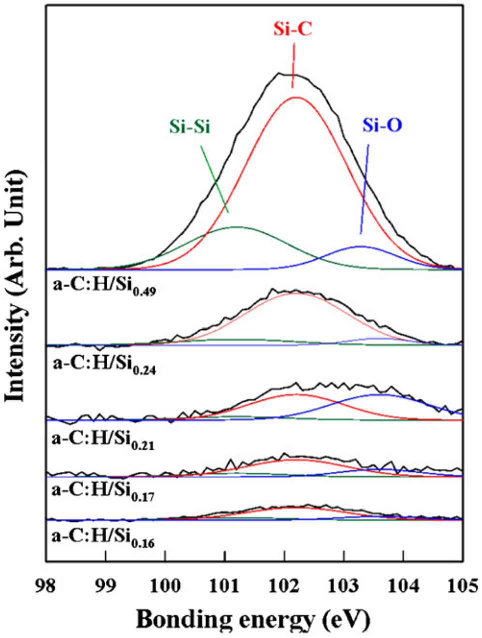

Fig. 6. XPS Si2p spectra of a-C:H/Si films with different Si contents.

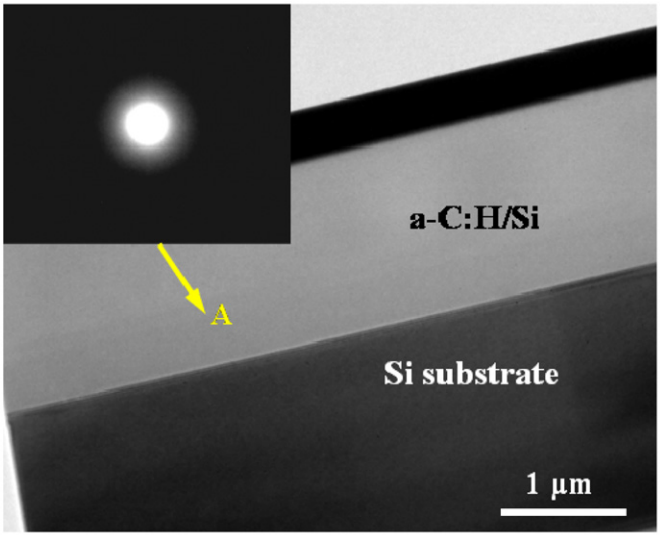

Fig. 7. Cross-sectional TEM bright field image and selected area diffraction pattern of a-C:H/$Si_{0.49}$ film.

a-C:H/Si film. In addition, the selected area diffraction (SAD) patterns taken from A (Fig. 7) in the film indicated that the film is amorphous. The Si–C and Si–Si bonds could only exist in a short-range order. Furthermore, the expected carbide precipitate was also not found. This was in contrast to the a-C:H films to which Cu and Ag had been added: such films had exhibited low solubility and low reactivity to carbon and contained segregated metallic clusters in their a-C:H matrices [9,10]. Thus, the Si introduced as a dopant was highly soluble in the a-C:H phase.

4. Conclusion

The microstructures of Si-incorporating a-C:H films having different Si contents and deposited by a hybrid technique comprising magnetron sputtering and plasma-enhanced chemical vapor deposition were investigated in this study. The Si content of the a-C:H films increased with an increase in the plasma power supplied. The fraction ratio of the sp^2 bonds also increased slightly with the increase in the plasma power and the Si content. However, owing to the target poisoning of the silicon electrode, the deposition rate for the films increased nonlinearly with the plasma power. Finally, although the Si contents of the films increased with the increase in the plasma power supplied, all the Si-incorporating a-C:H films synthesized in this study had an amorphous a-C:H structure and did not exhibit an observable secondary phase.

Acknowledgments

The authors would like to thank the Cathay General Hospital and Taipei Medical University for financially supporting this research under Contract no. 101CGH-TMU-03. In addition, we thank the researchers, Jing-Tang Chang and Ya-Chen Chang.

References

[1] P.K. Bachmann, R. Messier, Emerging technology of diamond thin films, Chemical and Engineering News 67 (1989) 24–39.

[2] K. Jia, Y.Q. Li, T.E. Fischer, B. Gallois, Tribology of diamond-like carbon sliding against itself, silicon nitride, and steel, Journal of Materials Research 10 (1995) 1403–1410.

[3] C. Jaoul, O. Jarry, P. Tristant, T. Merle-Mejean, M. Colas, C. Dublanche-Tixier, J.M. Jacquet, Raman analysis of DLC coated engine components with complex shape: understanding wear mechanisms, Thin Solid Films 518 (5) (2009) 1475–1479.

[4] A. Grill, Diamond-like carbon coatings as biocompatible materials—an overview, Diamond Related Materials 12 (2) (2003) 166–170.

[5] G. Dearnaley, J.H. Arps, Biomedical applications of diamond-like carbon (DLC) coatings: a review, Surface and Coating Technology 200 (7) (2005) 2518–2524.

[6] P. Yang, N. Huang, Y.X. Leng, J.Y. Chen, R.K.Y. Fu, S.C.H. Kwok, Y. Leng, P.K. Chu, Activation of platelets adhered on amorphous hydrogenated carbon (a-C:H) films synthesized by plasma immersion ion implantation–deposition (PIII-D), Biomaterials 24 (17) (2003) 2821–2829.

[7] J.W. Yi, M.W. Moon, S.F. Ahmed, H. Kim, T.G. Cha, H.Y. Kim, S.S. Kim, K.R. Lee, Long-lasting hydrophilicity on nanostructured Si-incorporated diamond-like carbon films, Langmuir 26 (22) (2010) 17203–17209.

[8] R.K. Roy, H.W. Choi, J.W. Yi, M.W. Moon, K.R. Lee, D.K. Han, J.H. Shin, A. Kamijo, T. Hasebe, Hemocompatibility of surface-modified, silicon-incorporated, diamond-like carbon films, Acta Biomaterials 5 (1) (2009) 249–256.

[9] H.W. Choi, J.H. Choi, K.R. Lee, J.P. Ahn, K.H. Oh, Structure and mechanical properties of Ag-incorporated DLC films prepared by a hybrid ion beam deposition system, Thin Solid Films 516 (2–4) (2007) 248–251.

[10] Y.H. Chan, C.F. Huang, K.L. Ou, P.W. Peng, Mechanical properties and antibacterial activity of copper doped diamond-like carbon films, Surface and Coating Technology 206 (6) (2011) 1037–1040.

[11] H.C. Cheng, S.Y. Chiou, C.M. Liu, M.H. Lin, C.C. Chen, K.L. Ou, Effect of plasma energy on enhancing biocompatibility of diamond-like carbon film with various titanium concentrations, Journal of Alloys and Compounds 477 (1–2) (2009) 931–935.

[12] R.K. Roy, H.W. Choi, S.J. Park, K.R. Lee, Sueface energy of the plasma treated Si incorporates diamond-like diamond carbon films, Diamond Related Materials 16 (9) (2007) 1732–1738.

[13] S.S. Camargo, A.L.B. Neto, R.A. Santos, F.L. Freire, R. Carius, F. Finger, Structural modifications and temperature stability of silicon incorporated diamond-like a-C:H films, Diamond Related Materials 7 (8) (1998) 1155–1162.

[14] F. Chai, N. Mathis, N. Blanchemain, C. Meunier, H.F. Hildebrand, Osteoblast interaction with DLC coated Si substrates, Acta Biomaterials 4 (5) (2008) 1369–1381.

[15] K. Baba, R. Hatada, S. Flege, W. Ensinger, Deposition of diamond-like carbon films on inner wall surfaces of millimeter-size-diameter steel tubes by plasma source ion implantation, IEEE Transactions on Plasma Science 39 (11) (2011) 3140–3143.

[16] S.C. Kim, K.Y. Lee, H.S. Lee, J.N. Kim, Synthesis of poly-substituted benzenes starting from Baylis–Hillman adducts: DBU-assisted unusual dehydrogenation, Tetrahedron 64 (1) (2008) 103–109.

[17] S.J. Dowey, K.M. Read, K.S. Fancey, A. Matthews, Performance analysis of coated tools in real-life industrial experiments using statistical techniques, Surface and Coating Technology 710 (1995) 74–75.

[18] C. Nørgård, S.S. Eskildsen, A. Matthews, The influence of nucleation density and oriented growth on the surface roughness of

diamond films, Surface and Coating Technology 74–75 (1995) 358–361.

[19] X.M. He, W.Z. Li, H.D. Li, Structure and properties of carbon nitride films, Surface and Coating Technology 84 (1–3) (1996) 414–416.

[20] J. Deng, M. Braun, DLC, multilayer coatings for wear protection, Diamond Related Materials 4 (1995) 936–943.

[21] N.A. Sánchez, C. Rincón, G. Zambrano, H. Galindo, P. Prieto, Characterization of diamond-like carbon (DLC) thin films prepared by r.f. magnetron sputtering, Thin Solid Films 373 (1–2) (2000) 247–250.

[22] D.Y. Wang, K.W. Weng, C.L. Chang, X.J. Guo, Tribological performance of metal doped diamond-like carbon films deposited by cathodic arc evaporation, Diamond Related Materials 9 (3–6) (2000) 831–837.

[23] V.N. Inkin, G.G. Kirpilenko, A.A. Dementjev, K.I. Maslakov, A superhard diamond-like carbon film, Diamond Related Materials 9 (3–6) (2000) 715–721.

[24] R.F. Huang, C.Y. Chan, C.H. Lee, J. Gong, K.H. Lai, C.S. Lee, K.Y. Li, L.S. Wen, C. Sun, Wear-resistant multilayered diamond-like carbon coating prepared by pulse biased arc ion plating, Diamond Related Materials 10 (9–10) (2001) 1850.

[25] V.N. Inkin, G.G. Kirpilenko, A.J. Kolpakov, Internal stresses in Ta–C films deposited by pulse arc discharge method, Diamond Related Materials 10 (3–7) (2001) 1103–1108.

[26] W.C. Feng, C.H. Wang, H.C. Cheng, S.Y. Chiou, C.S. Chen, K.L. Ou, Enhancement of hemocompatibility on titanium implant with titanium-doped diamond-like carbon film evaluated by cellular reactions using bone marrow cell cultures in vitro, Journal of Vacuum Science and Technology B 27 (3) (2009) 1559–1565.

[27] L.L. Wu, B.C. Holloway, D.P. Beesabathina, C. Kalil, D.M. Manos, Analysis of diamond-like carbon and Ti/MoS_2 coatings on Ti–6Al–4V substrates for applicability to turbine engine applications, Surface and Coating Technology 130 (2–3) (2000) 207–217.

[28] G. Capote, L.G. Jacobsohn, M.D. Michel, C.M. Lepienski, A.L. Vieira, D.F. Franceschini, Diamond Related Materials 16 (3) (2007) 616.

[29] S.C. Ray, T.I.T. Okpalugo, P. Papakonstantinou, C.W. Bao, H.M. Tsai, J.W. Chiou, J.C. Jan, W.F. Pong, J.A. McLaughlin, W.J. Wang, Electronic structure and hardening mechanism of Si-doped/undoped diamond-like carbon films, Thin Solid Films 482 (1–2) (2005) 242–247.

[30] T. Iseki, H. Mori, H. Hasegawa, H. Tachikawa, K. Nakanishi, Structural analysis of Si-containing diamond-like carbon, Diamond Related Materials 15 (4–8) (2006) 1004–1010.

[31] F. Zhao, H.X. Li, L. Ji, Y.J. Wang, Y.F. Mo, W.L. Quan, Q.H. Kong, Y.X. Wang, J.M. Chen, H.D. Zhou, Microstructure and mechanical properties of graphitic a-C:H:Si films, Surface and Coating Technology 206 (16) (2012) 3467–3471.

[32] F.C. Tai, S.C. Lee, C.H. Wei, S.L. Tyan, Correlation between ID-IG ratio from visible Raman spectra and sp2/sp3 ratio from XPS spectra of annealed hydrogenated DLC film, Materials Transactions 47 (7) (2006) 1847–1852.

[33] J. Robertson, Properties of diamond-like carbon, Surface and Coating Technology 50 (3) (1992) 185–203.

[34] I. Bertoti, A. Toth, M. Mohai, J. Szepvolgyi, Chemical structure and mechanical properties of Si-containing a-C:H and a-C thin films and their Cr and W-containing derivatives, Surface and Coating Technology 206 (4) (2011) 630–639.